J. Fluid Mech. (1994), *vol.* 265, *pp.* 289–302

The observation of the simultaneous development of a long- and a short-wave instability mode on a vortex pair

By P. J. THOMAS[1] AND D. AUERBACH[2]

[1] Department of Applied Mathematics and Theoretical Physics, University of Cambridge, Silver Street, Cambridge, CB3 9EW, UK

[2] Max-Planck-Institut für Strömungsforschung, Bunsenstr. 10, D-37073 Göttingen, Germany

(Received 21 July 1993 and in revised form 18 October 1993)

Experiments on the stability of vortex pairs are described. The vortices (ratio of length to core diameter L/c of up to 300) were generated at the edge of a flat plate rotating about a horizontal axis in water. The vortex pairs were found to be unstable, displaying two distinct modes of instability. For the first time, as far as it is known to the authors, a long-wave as well as a short-wave mode of instability were observed to develop simultaneously on such a vortex pair. Experiments involving single vortices show that these do not develop any instability whatsoever. The wavelengths of the developing instability modes on the investigated vortex pairs are compared to theoretical predictions. Observed long wavelengths are in good agreement with the classic symmetric long-wave bending mode identified by Crow (1970). The developing short waves, on the other hand, appear to be less accurately described by the theoretical results predicted, for example, by Widnall, Bliss & Tsai (1974).

1. Introduction

An outstanding feature of many vortices met in nature (e.g. tornadoes, tornadic thunderstorms, highs and lows, to name but a few) is their remarkable persistence. The same applies to certain vortices which we generate wittingly or unwittingly (e.g. wake vortices, turbulent vortex rings). It was Kelvin who was able to show that single columnar vortices were stable to perturbations along the column (bending wave instability), thereby giving the above experience its first theoretical foundation. However, since Kelvin's seminal work at least four other regions of interest have developed in which stability is often the exception rather than the rule. The first two, the stability of a rolling-up vortex sheet and the stability of some configurations of vortices (e.g. the Kármán vortex street), are both essentially two-dimensional instabilities and will not concern us in this paper. The other two are related to Kelvin's three-dimensional instabilities: a long-wave and a short-wave instability mode. The long-wave mode with wavelengths much larger than the vortex core diameter c is named after Crow (1970). This instability mode develops along a pair of initially straight parallel vortices when the destabilizing effect of the strain field induced by one of the two vortices on its neighbour overcomes the stabilizing influence of its own self-induced motion. In his paper Crow also identified a short-wave mode of instability with a wavelength comparable with the core diameter but stated that only the long-wave mode is observed in practice. Widnall, Bliss & Tsai (1974) recognized that the short-wave mode as identified by Crow was spurious, but were able to show (Widnall *et al.* 1974; Widnall 1975; Tsai & Widnall 1976) that a short-wave mode of instability

does indeed exist for vortices with a more complex radial velocity structure than assumed in Crow's simple model.

In the meantime many details of the above problem have been uncovered, showing its complexity and the care required in comparing the often very idealized theories with the few known experiments. These details include, for example, the effects of axial stretching (e.g. Klein, Majda & McLaughlin 1992 for single vortices and Marshall 1992 for pairs) and axial flow (e.g. Marshall 1993), as well as the existence of unstable modes substantially smaller than the core diameter (Landman & Saffman 1987). It should be noted that the important aspect of the influence of axial flow on the vortex stability still largely remains an unanswered question. However, the axial flow is found to influence the wave speed in the case of the long waves (Saffman 1992). In relation to the short waves the influence of axial flow has only been investigated for the case when it is small, such that it can be treated as a perturbation in the theoretical analysis. For this case it is found that the instability persists and that the band of unstable wavenumbers remains unchanged, whereas the wave from which the most unstable disturbance arises is altered (see Saffman 1992, p. 249). We need not give an extensive survey of the theoretical work that has been carried out on vortex stability over the last twenty years as an excellent and detailed account of this work has very recently been published by Saffman (1992). Moreover, our own measurements of the relevant details of the vortex structure are of too qualitative a nature to allow comparison with these theories.

In contrast to the relatively large number of theoretical publications on vortex stability, quantitative experimental results concerning straight line vortices up to the present day seem rather scarce. Most attention in the experimental field has focused on the stability of vortex rings which are relatively easy to generate in the laboratory. Vortex rings were studied in detail, for instance, by Maxworthy (1972, 1974, 1977) and Didden (1977) and even as early as 1939 in the classic study by Krutzsch (1939) whose photographs probably presented the first experimental evidence for the instability of vortex rings.

The only quantitative experimental data that Crow (1970) had readily available in order to verify his findings concerning the wavelength of the waves that appear on a pair of interacting vortices were the well-known photographs by Smith & Beesmer (1959), reproduced by Van Dyke (1982), showing a growing instability on a pair of trailing vortices behind the wings of an airplane. Estimating the wavelength of these waves, Crow found good agreement with the predictions of his long-wave theory. He did, however, state that owing to the crudeness of the estimate this agreement might be partly fortuitous.

There appear to be no other experimental laboratory data available that can help to check the validity of Crow's theoretical results on a broader basis and that can also be used to check the short-wave predictions of, for example, Widnall *et al.* for a pair of straight line vortices. The purpose of the present study is thus twofold. First, we document the simultaneous development of a long-wave mode as well as a short-wave mode of instability on a vortex pair, which to our knowledge has not previously been observed. Second, we present some quantitative data that can be used to test Crow's long-wave theory and Widnall *et al.*'s short-wave theory.

2. Experimental set-up

The vortex pairs investigated in this study were generated at one edge – the apex of a wedge-shaped brass extension – of a flat 20 mm thick Perspex plate rotated about a horizontal axis in water (figure 1). When the plate is initially set into rotation a starting

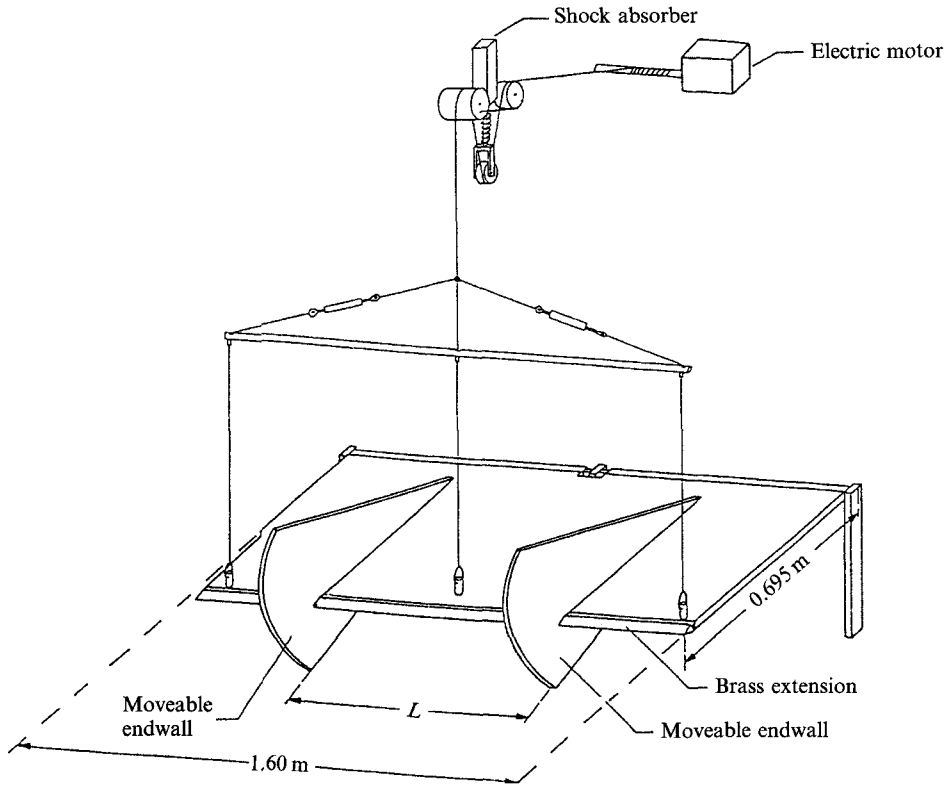

FIGURE 1. Sketch of the experimental set-up.

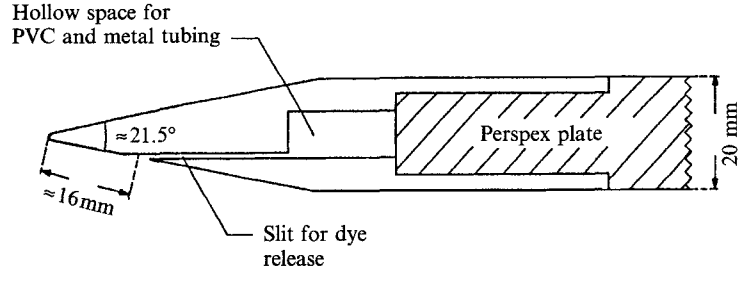

FIGURE 2. Sketch of the brass wedge attached to the Perspex plate.

vortex is generated along the outer edge. Stopping the plate shortly thereafter (approximately 1–2 s) generates the second vortex of the pair, a stopping vortex. The vortices were bound at their ends by two moveable Perspex endwalls slid onto the plate, allowing a variable vortex length of up to $L = 1.4$ m. The plate was mounted inside a $1 \times 1 \times 2$ m water tank.

The plate was rotated upwards by means of a drawing mechanism consisting of a variable-speed electric motor whose extended axis wound up a thin wire rope attached to the plate. The wire was threaded through a pulley attached to a shock absorber in order to minimize motor-induced vibrations of the plate.

The vortices were visualized using a neutrally buoyant dye mixture consisting of water, ink and alcohol. The dye was released through a 1 mm wide slit on the bottom side of the plate's wedge-shaped, brass extension (see figures 1 and 2). The dye could be released either along the entire length of the vortex generating edge or, alternatively,

after sealing certain areas of the slit at chosen single locations only. The dye was fed into and distributed inside the inner part of the brass wedge by means of a tubing system lead along one of the plate's radial edges and originating from a reservoir situated above the tank.

The rotation rate of the plate could be monitored for different speeds of the drawing mechanism's electric motor. The vortex pairs investigated here were generated for two different rotation rates ω_p of the plate of $\omega_p \approx 2.2 \times 10^{-2}$ rad s^{-1} (referred to as I) and $\omega_p \approx 4.2 \times 10^{-2}$ rad s^{-1} (referred to as II). The initial acceleration phase took less than 0.5 s. The length L of the vortices, was varied between $L = 40$ and 140 cm. Details of the starting procedure as well as the trajectory of the starting vortex prior to stopping the plate have been studied and modelled in detail (Thomas 1988). The vortices were photographed on slides using motor-driven 35 mm cameras at a frequency of approximately four frames per second.

3. Experimental results

Figure 3 shows one of the investigated vortex pairs at $t \approx 0.8$ s after stopping the plate. The vortex pair was viewed from the side of the tank, i.e. looking through the endwalls and parallel to the axes of the two vortices. In this instance the vortex pair was visualized by marking it with dye only at one single location along the edge approximately halfway between the endwalls. Note that the bottom vortex (starting vortex) is not quite as well marked by the dye as the upper vortex (stopping vortex). This is due to the dye outlet being located at the bottom side of the plate's brass extension. In its mutually induced velocity field the vortex pair translates (with a velocity u through the surrounding fluid) radially away from the plate, which points slightly upwards after it is stopped. In figure 3 the vortex pair can be seen to have moved about 5 cm away from the edge of the wedge. Figure 4(*a–e*) shows the temporal evolution of a section of one such vortex pair seen in a direction perpendicular to the axes of the vortices (with the vortex pair approaching the viewer). The section shown in the figures is approximately 25 cm long and originates from a location in the vicinity of the plate's midplane. The total length of the pair in this case was $L = 120$ cm. The dark area at the bottom of each of the pictures of figure 4 is part of the wedge, and a bit of the wire rope of the drawing mechanism and its attachment to the plate can also be seen to the left of each picture. In figure 4(*a*) at $t \approx 0.4$ s after stopping the plate only the upper vortex, the stopping vortex, can be clearly identified. The bottom vortex, the starting vortex, is obscured by the plate's extension in the background. The axis of the stopping vortex can be seen to be initially straight. In figure 4(*b*) at $t \approx 0.8$ s both vortices are now visible as the vortex pair has moved further away from the edge of the plate. Nevertheless, the starting vortex is less well marked by the dye. Whereas no clear wavelengths can be identified yet, first indications of vortex deformation have become visible on the stopping vortex. A clear deformation of the stopping vortex has occurred by $t \approx 1.3$ s in figure 4(*c*). A long-wave mode of instability as well as a simultaneously developing short-wave mode of instability can clearly be identified. The starting vortex appears to be more stable in the velocity field of the stopping vortex and no obvious deformation of its core is visible. On the stopping vortex one can clearly see that the waves of the core and those of the outer vortex are in antiphase, similar to the ring vortex case. At $t \approx 1.7$ s in figure 4(*d*) the amplitudes of both the long waves and the short waves on the stopping vortex have grown further. The starting vortex, however, continues to appear less affected by the presence of the stopping vortex, showing no apparent deformation. By $t \approx 2.1$ s in figure 4(*e*) the stopping vortex has started to

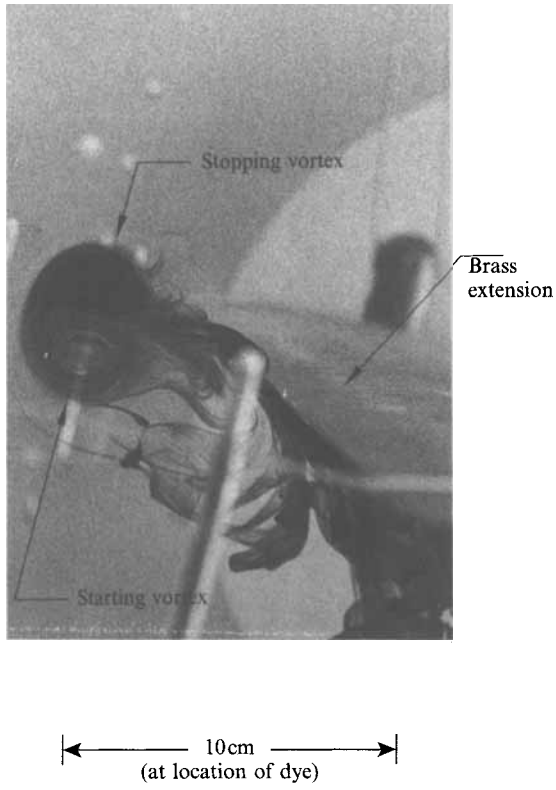

FIGURE 3. A vortex pair moving away from the wedge viewed parallel to the vortices' axes.

decay, whereas the starting vortex still shows no clear indication of either deformation or decay. The likely reason for only the stopping vortex developing clear and distinguishable wavy deformations in figure 4 should probably be attributed to the mechanisms of the generation of the vortex pair, as the stopping vortex is formed under the influence of the already existing, fully developed velocity field of the starting vortex. The numerical values of the wavelengths for both instability modes as well as the values of other relevant quantities for the various runs of the experiment as obtained from the photo sequences of the development of the vortex pairs are documented in table 1. Assuming a two-dimensional pair we can define the vortex Reynolds number Re as Γ/ν where Γ is obtained from the data of table 1 using the expression $u = \Gamma/(2\pi b)$. Hence, the Reynolds number for the pairs generated with rotation rate I of the plate is found to be in the range of 2000–5000 and for the pairs generated with rotation rate II in the range of 5000–12000.

Figures 5 and 6 show the temporal development of the distance b between the centres of the two vortices of a pair, the long wavelengths λ_l and the short wavelengths λ_s for pairs of various lengths and generated with the two different rotation rates ω_p (I and II). The error involved in the measurement of b is some 3 mm. The average wavelengths for both instability modes were obtained as the ratio of the length of a portion of the vortex pair and the total number of waves developing on that portion, rather than measuring each single wave separately. It can be seen that the only tendency visible in figures 5 and 6 is that the distance b (figure 5) appears to increase with time. Neither of the wavelengths, λ_l (figure 6*a*) nor λ_s (figure 6*b*), shows any clear temporal variation.

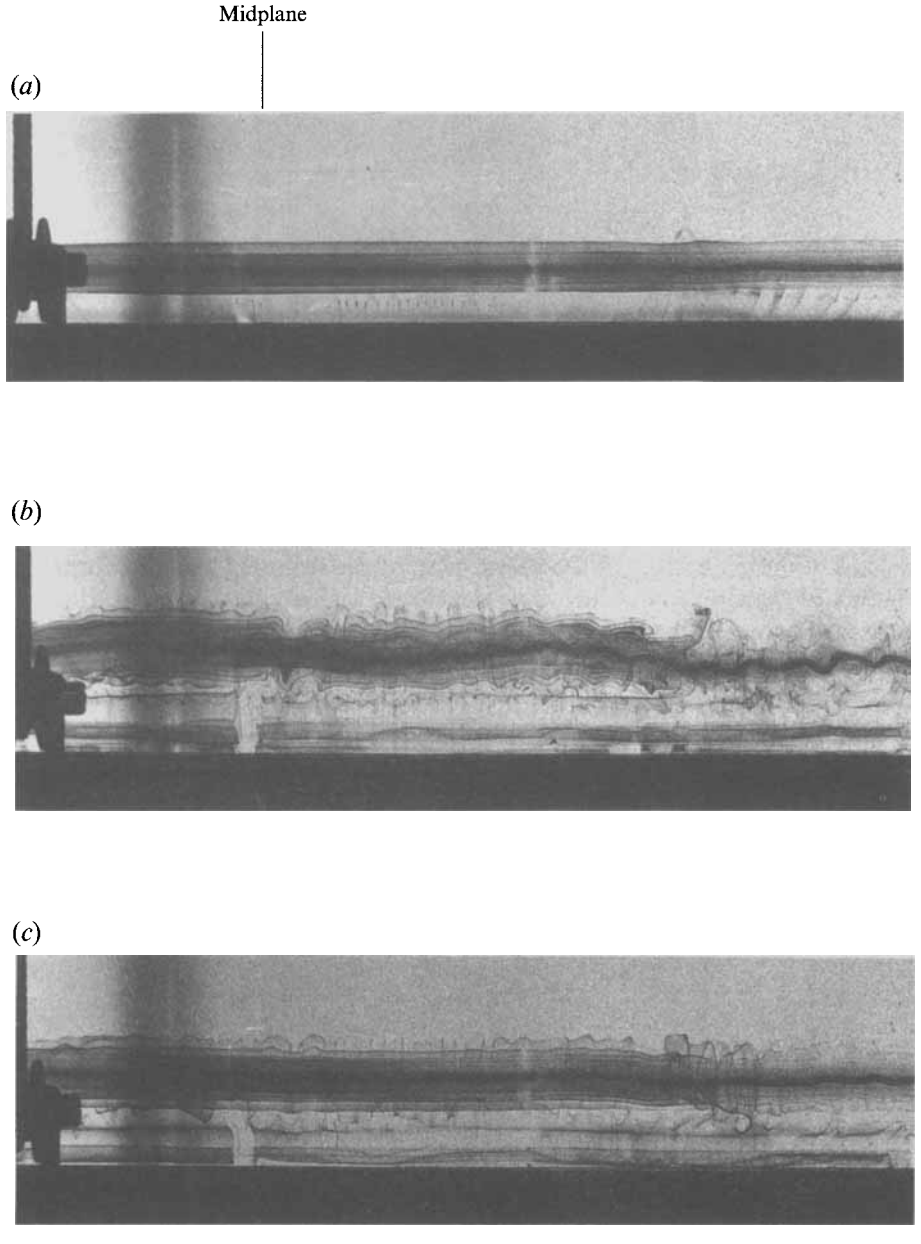

FIGURE 4(*a–c*). For caption see facing page.

The increase of the distance b between the centres of the two vortices of a vortex pair implies that hitherto quiescent fluid has been entrained into the pair's recirculation cell. For vortex rings Maxworthy (1974, 1977) showed that entrainments $E = \Delta b / \int u \, dt$ (with Δb representing the radius of the vortex ring in Maxworthy's study) of between 10^{-3} and 10^{-2} occurred, where the integral in the denominator is the distance travelled by the vortex during the time in which the size increases by Δb. We can obtain an estimate of the entrainment rate for the vortex pairs of the present study. From the data displayed in figure 5 one can determine an average temporal growth of b for each of the two rotation rates of the plate; one finds $\Delta b / \Delta t \approx 0.25$ cm s^{-1} for rotation rate

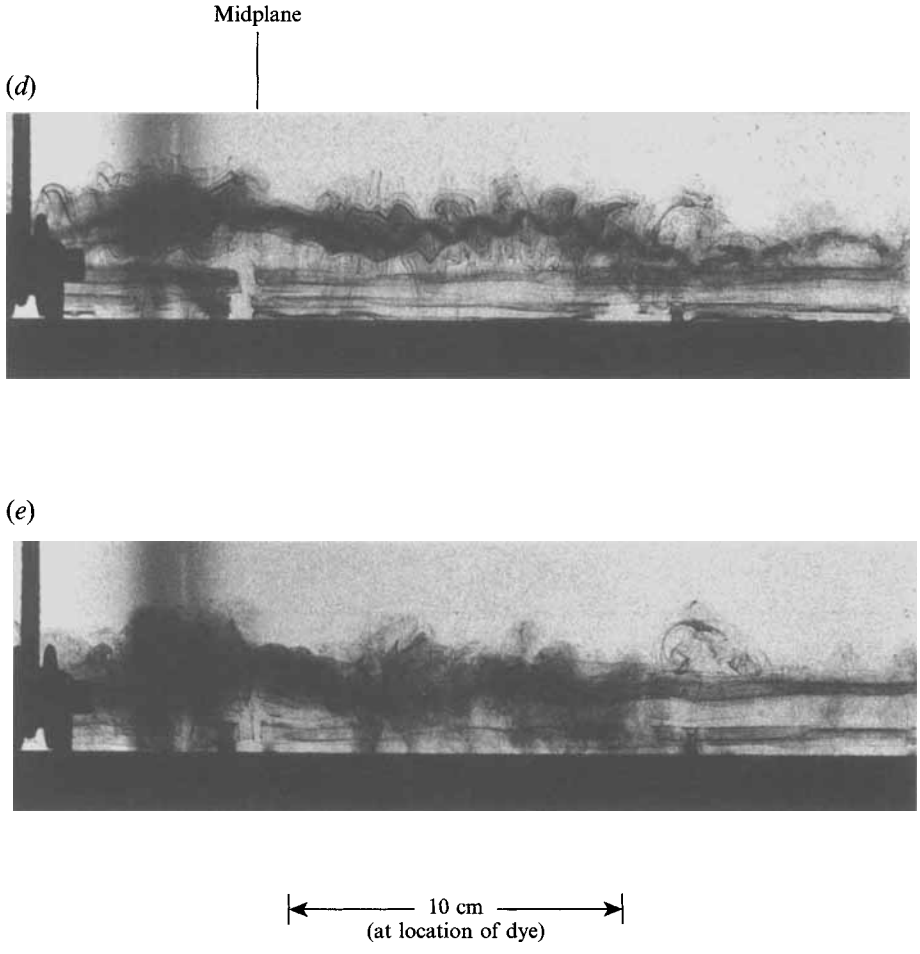

FIGURE 4. Temporal evolution of some 25 cm of a vortex pair with a total length of $L = 120$ cm, viewed approximately halfway between the bounding endwalls. View perpendicular to that of figure 3. (*a*) $t \approx 0.4$ s, (*b*) $t \approx 0.8$ s, (*c*) $t \approx 1.3$ s, (*d*) $t \approx 1.7$ s, (*e*) $t \approx 2.1$ s.

I and $\Delta b/\Delta t \approx 0.5$ cm s^{-1} for rotation rate II. From the data of table 1 we obtain two constant average values for the velocity u of the vortex pairs during the runs of the experiment as $u \approx 2.5$ cm s^{-1} for rotation rate I and $u \approx 6.3$ cm s^{-1} for rotation rate II. From this one arrives at entrainment rates $E \approx 0.1$ for rotation rate I and $E \approx 0.08$ for rotation rate II. These values are distinctly larger than the values stated by Maxworthy for ring vortices. Our present result is consistent with an estimate we obtained from the investigation of Barker & Crow (1977) who studied the motion of a vortex pair impinging on a wall. From their figure 8 and for times $t \lesssim 4$ s, i.e. before wall effects actually become significant in their experiments one finds $E \approx 0.2$, similar to our values. The fact that the entrainment is approximately one order of magnitude larger for vortex pairs than for ring vortices may reflect the different structures of the recirculation cells of rings and pairs. As Barker & Crow's vortex pairs ($L \approx 15$ cm, $b \approx 12$ cm) did not develop any of the instabilities discussed in the present study we can moreover conclude that the growing instabilities observed here do not have a significant influence on the entrainment behaviour of vortex pairs.

The effect of changing the vortex length L on the wavelengths λ_l and λ_s of the

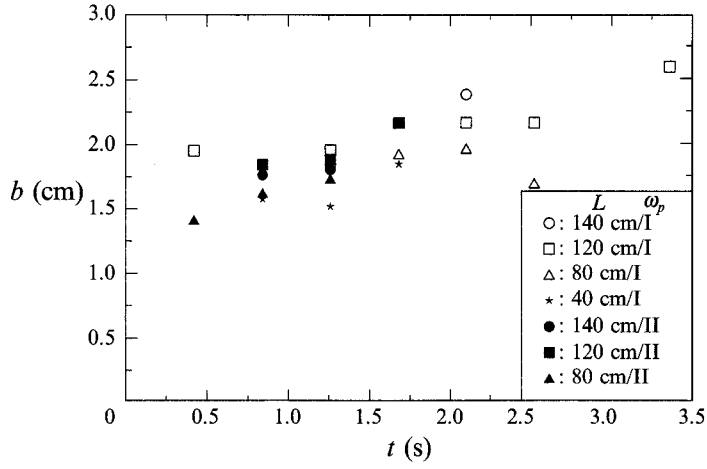

FIGURE 5. The distance b between the centres of the two vortices of a vortex pair as a function of the time t for the two rotation rates ω_p (I and II) of the plate.

L (cm)	t (s)	b (cm)	λ_l (cm)	λ_s (cm)	u (cm s^{-1})	(β_{th}/β) long	(β_{th}/β) short
			Rotation rate I				
140	1.26	1.84	*	1.41	2.77	*	3.10
140	1.68	2.16	17.43	1.37	2.39	0.94	2.56
140	2.10	2.38	15.66	1.42	2.26	0.76	2.41
120	0.42	1.95	*	1.41	2.51	*	2.92
120	1.26	1.95	*	1.59	2.51	*	3.30
120	1.68	2.16	10.30	1.22	2.33	0.55	2.28
120	2.10	2.16	11.28	*	2.14	0.61	*
120	2.52	2.16	17.07	1.21	2.51	0.92	2.26
120	3.36	2.59	16.58	1.51	2.51	0.74	2.36
80	1.68	1.92	*	1.27	1.80	*	2.67
80	2.10	1.96	13.10	1.29	2.20	0.78	2.66
80	2.52	1.69	*	1.23	1.99	*	2.94
40	0.84	1.57	*	0.93	2.51	*	2.39
40	1.26	1.51	*	1.00	3.04	*	2.68
40	1.68	1.84	*	0.79	3.52	*	1.74
			Rotation rate II				
140	0.84	1.76	*	1.44	4.84	*	3.31
140	1.26	1.80	14.95	1.37	4.84	0.96	3.08
120	0.84	1.84	*	1.10	6.54	*	2.42
120	1.26	1.88	16.79	1.44	6.41	1.04	3.10
120	1.68	2.16	*	1.41	6.03	*	2.64
80	0.42	1.41	*	0.93	8.30	*	2.67
80	0.84	1.62	7.40	1.36	7.71	0.53	3.39
80	1.26	1.73	13.50	1.57	6.03	0.91	3.67

TABLE 1. Summary of the vortex pair data

developing instability modes is displayed in figures 7(a) and 7(b), respectively. The trend for the wavelength λ_l to increase with L (figure 7a) is clearer than for the wavelength λ_s (figure 7b). In the case of the short waves only the value of the wavelength for the shortest vortex pair with $L = 40$ cm seems to be somewhat smaller

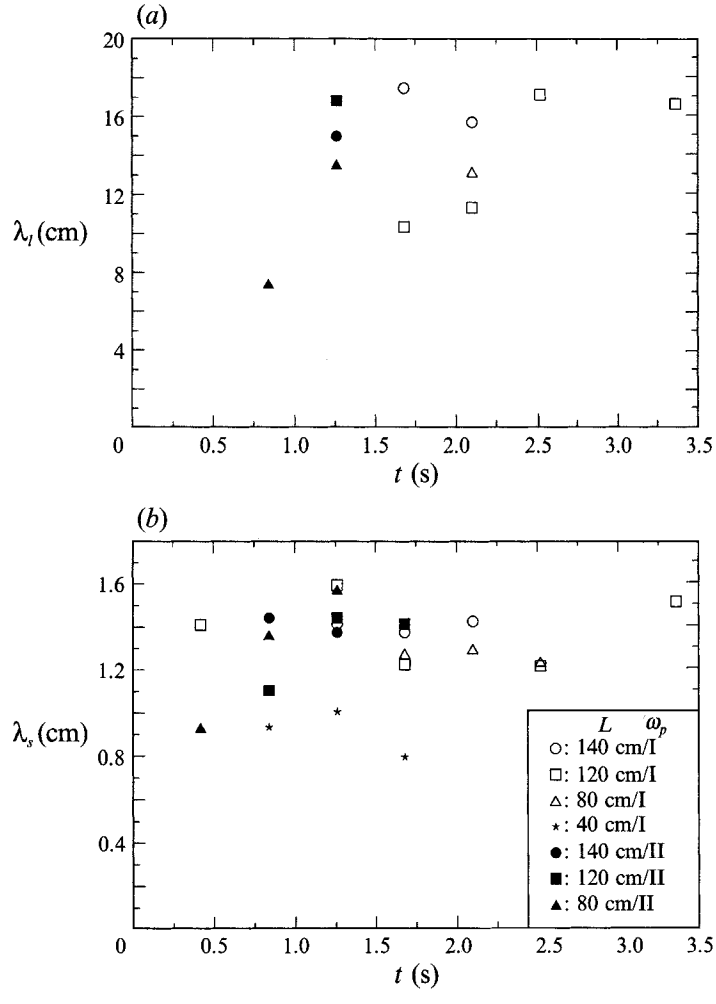

FIGURE 6. (*a*) The wavelength λ_l of the long-wave mode of instability and (*b*) the wavelength λ_s of the short-wave mode of instability, as a function of the time t for the two rotation rates ω_p (I and II) of the plate.

than the wavelengths obtained for larger values of L. How does a change in the rotation rate effect the wavelengths? Figures 5–7 do not show any significant dependence of the rotation rate ω_p on the results obtained. The experiments were carried out as described above for the two different rotation rates of the plate and the wavelengths were registered the moment the waves' amplitudes were clearly discernable. As can be seen in figures 6(*a*) and 6(*b*) there is a trend for the time of first registration of the wavelengths to be somewhat earlier for the higher rotation rate II than in the case of the lower rotation rate I. This grouping of the data might indicate a dependence of the amplification rate of the developing instabilities on the plate's rotation rate, i.e. the amplification rate being larger for higher rotation rates. However, this conclusion has to be viewed with some care. Since we could not determine the rotation rate of the plane on which the waves grew, the amplitudes seen, for example in figure 4, do not necessarily reflect the true amplitude. Moreover, an alternative explanation for the observed grouping of the data might be some disturbances due to large-scale fluid motion at higher plate velocities.

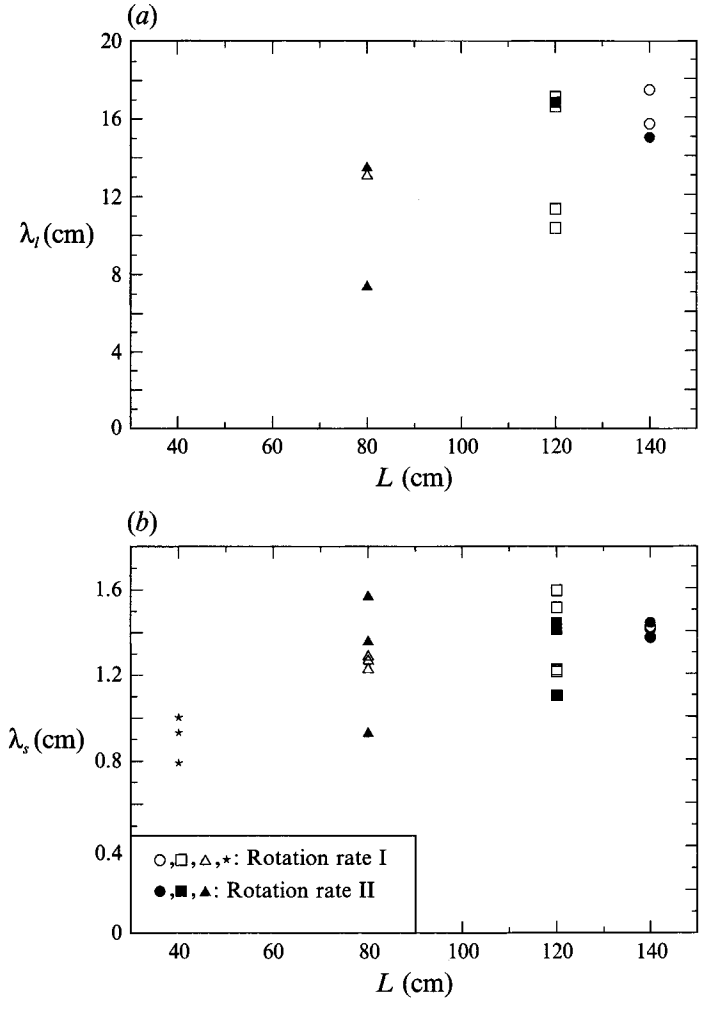

FIGURE 7. (*a*) The wavelength λ_l of the long-wave mode of instability and (*b*) the wavelength λ_s of the short-wave mode of instability, as a function of the vortex length L for the two rotation rates ω_p (I and II) of the plate.

One might expect the growth rate of the instability to increase with increasing rotation rate, which just means that the larger the strain rate induced by one vortex on its neighbour, the larger the growth rate. Nevertheless, the growth rate also depends on the vortex core size, its velocity distribution, the difference between the Kelvin mode and the excited mode (Widnall & Tsai 1977) and the axial flow. Hence the above observation should not be regarded as trivial. Regarding the effect of the axial flow, it should be pointed out that no axial flow other than self-induced axial flow was present in the experiments. This self-induced axial flow was observed to be generated at the endwalls and is directed towards the centre, with developing local flow velocities of up to 1.7 times the linear velocity of the edge of the Perspex plate. The axial flow occurs, however, for times which are of the magnitude of the running times of the present experiments localized to the endwalls and it is negligible in the region observed here (Thomas 1988).

Before comparing the above experimental results for the wavelengths of the developing instability modes on a vortex pair to theoretical predictions it seems

relevant to remark on the stability of single vortices. Additional experiments, not discussed here, were carried out in which the generation time of the starting vortex was large enough to allow the observation of this single vortex as it grew. None of the single vortices investigated showed any sign whatsoever of the development of an instability (Thomas 1988). This indicates that the instabilities observed above depend crucially on the proximity of two vortices in their mutually induced velocity field rather than being a property of just one single vortex.

4. Prediction of the wavelengths that appear and comparison with experimental data

Mechanisms leading to the growth of waves on vortices were enumerated in the introduction. On the basis of the above result – that single vortices appear stable – it would only seem necessary to consider vortex interaction models such as those of Crow (1970), Widnall *et al.* (1974) and Widnall (1975). To obtain a prediction of the wavelengths of the most rapidly growing wave modes of instability from these theories an estimate of the ratio of the separation b between the centres of the vortices to the core diameter c of the vortices of the vortex pair is needed. Such an estimate was obtained by Spreiter & Sacks (1951) for the case of a pair of trailing vortices behind an elliptically loaded wing and is approximately given by

$$b/c = 5. \tag{1}$$

For the case of ring vortices this result was confirmed by Didden (1977) with the ring diameter in his study replacing the separation b. If it is assumed that the above numerical value also holds for the vortices generated in the present study then it follows from the analysis of Crow (1970) that these vortices should show a developing symmetric long-wave instability with a dimensionless wavenumber β_{th} according to

$$\beta_{th} = \frac{2\pi}{\lambda_{th}} b \approx 0.73. \tag{2}$$

The quantity $2\pi/\lambda_{th}$ is the relevant wavenumber. The expected wavelength of the long-wave mode is thus

$$\lambda_{th} \approx 8.6\, b. \tag{3}$$

The wavelength of the instability predicted by Widnall *et al.* (1974) depends on the exact radial velocity structure of the vortex core and the vorticity distribution across the core. However, the upper limit of the wavelength predicted is obtained for their second radial bending mode and is given by

$$\frac{2\pi}{\lambda_{th}} \frac{c}{2} \approx 2.5. \tag{4}$$

Using the estimate (1) for the core diameter c yields

$$\beta_{th} = \frac{2\pi}{\lambda_{th}} b \approx 25.0. \tag{5}$$

The expected upper wavelength limit of the short-wave mode is thus

$$\lambda_{th} \approx 0.25\, b. \tag{6}$$

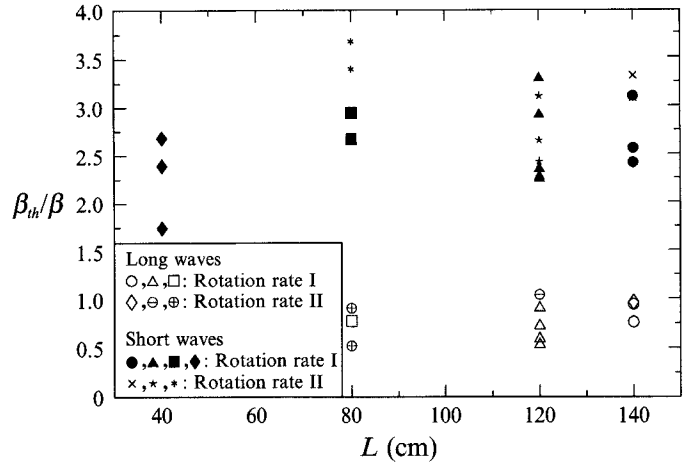

FIGURE 8. The ratio of the predicted dimensionless wavenumber and the relevant experimental value $\beta_{th}/\beta = \lambda/\lambda_{th}$ as a function of the vortex length L for the long- and the short-wave mode of instability for the two rotation rates ω_p (I and II) of the plate.

Figure 8 shows how the theoretical predictions compare with the present experimental results. In figure 8 the ratios of the predicted dimensionless wavenumbers β_{th} ((2) and (5)) and their respective experimental values $\beta = (2\pi/\lambda)b$, where λ represents the measured, averaged wavelength for the long (λ_l) and short (λ_s) wave instability modes respectively (see table 1), are plotted as a function of the vortex length L. The ordinate of figure 8 hence represents the ratio of the experimentally obtained wavelengths to the predicted wavelengths. The error may be as large as 20% and is primarily caused by the error in b mentioned earlier. As can be seen the long waves are in general better predicted by the Crow theory than are the short waves by the Widnall theory (note that owing to scaling the errors for the long-wave instability seem smaller than what they really are). The wavelength of the long-wave instability mode observed during the experiments was on average about 15%–20% shorter than predicted by Crow. The developing short waves, on the other hand, are found to be around 200% longer than the upper wavelength limit obtained from Widnall *et al.* (1974) for their second radial bending mode. (It should be noted that the short-wave data agree better with Crow's short-wave result which predicts $\lambda_{th} = 0.37b$, although this has to be considered a coincidence.) If the data for β_{th}/β were plotted as a function of t rather than L as in figure 8 one would see that the agreement between experimental and theoretical data does not change significantly with time for the long waves. The agreement for the short waves on the other hand shows a trend to improve somewhat for larger values of t with the wavelengths initially being around 200% longer than predicted and around 150% longer for the later stages.

5. Conclusions

Experiments on the stability of vortex pairs were described. Each pair, consisting of two initially straight long vortices, was generated at one edge of a flat Perspex plate rotated about a horizontal axis in water: when the plate was set into rotation a starting vortex was generated; when it was stopped, a stopping vortex was generated. A short and a long bending wave instability were amplified simultaneously along the entire length of the stopping vortex. Additional experiments with single vortices revealed

these to be surprisingly stable with no instabilities developing whatsoever. The developing instability modes observed on the vortex pairs thus seem to depend crucially on the interaction of the two vortices of a pair in their mutually induced velocity field. The wavelengths λ_l and λ_s of the long- and the short-wave instability modes remained approximately constant with time. The wavelength of the short waves seemed to be independent of the vortex length L whereas the wavelengths of the long waves tended to grow with the vortex length for the range of values of L investigated. Assuming that the plane in which the waves grow – if indeed they are in a single plane – does not effectively rotate (an aspect which we could not measure), the experimental data indicate that the amplification rate of both instability modes increases with the rotation rate of the plate, i.e. the plate's edge velocity. The wavelengths of the developing instabilities were compared with theoretical predictions. The observed long waves were some 15%–20% shorter than predicted by Crow (1970). The observed short waves, on the other hand, are less accurately described by theoretical models, as for example by the model of Widnall *et al.* (1974), and were found to be some 200% longer than predicted. Finally, entrainment into the recirculation cell of the investigated pairs was found to be approximately one order of magnitude larger than the corresponding value for the case of vortex rings; the entrainment behaviour of the vortex pairs seems moreover not to be significantly affected by the growing instabilities.

The observation that the wavelength λ_l of the long waves shows a trend to increase with increasing vortex length L while no such behaviour is apparent for the wavelength λ_s of the short waves can be explained qualitatively if one considers that the theoretical analyses are based upon the assumption of infinitely long vortices. If this requirement is not satisfied the dynamics will depend on the exact boundary conditions at the endwalls and the vortex length L will enter into the problem. However, as the long waves are approximately ten times longer than the short waves the requirement for the infinitely long vortices will be effectively satisfied in the case of the short waves for considerably smaller values of L than in the case of the long waves. From this it can also be understood why in figure 7(*b*) only the short waves for the case with $L = 40$ cm are apparently somewhat shorter than for the runs of the experiment with $L > 40$ cm where, on average, they appear to be constant.

In the experiments it was observed that in most cases only one of the vortices of a pair developed clearly identifiable wavy deformations. The vortices were generated by starting the plate and then stopping it again after a short time interval. Thus, the two vortices of a pair were not generated at the same instant and are hence in slightly different stages of their evolution during the experiment. Owing to this generation process the stopping vortex, which always showed the clearest and most distinguishable wavy deformations, is created while the velocity field of the starting vortex is already present and acting on the developing stopping vortex. Hence, it could be argued that the models employed to obtain predictions for the wavelengths of the waves developing on the vortex pair are not strictly applicable for the present experimental situation and that both the good agreement of the wavelengths of the observed long waves as well as the rather worse agreement for the short waves with their theoretical predictions are fortuitous. Moreover, the estimate of the ratio of the separation b and the vortex core diameter c of the vortices, given by (1) was assumed from earlier studies cited above rather than measured for the vortex pairs investigated in this study. Although the agreement between the numerical value given by these earlier studies for two substantially different flow situations suggests that this value might also be a good estimate for the present study, this result needs to be experimentally checked for the above experimental situation.

REFERENCES

BARKER, S. J. & CROW, S. C. 1977 The motion of two-dimensional vortex pairs in a ground effect. *J. Fluid Mech.* **82**, 659–671.

CROW, S. C. 1970 Stability theory for a pair of trailing vortices. *AIAA J.* **8**, 2172–2179.

DIDDEN, N. 1977 Untersuchung laminarer, instabiler Ringwirbel mittels Laser-Doppler-Anemometrie. *Mitt. aus dem MPI für Strömungsforschung und der AVA*, Nr. 64, *Göttingen, Germany.*

FUKUMOTO, Y. & MIYAZAKI, T. 1991 Three-dimensional distortions of a vortex filament with axial velocity. *J. Fluid Mech.* **222**, 369–416.

KLEIN, R., MAJDA, A. J. & MCLAUGHLIN, R. M. 1992 Asymptotic equations for the stretching of vortex filaments in a background flow field. *Phys. Fluids* A **4**, 2271–2281.

KRUTZSCH, C. H. 1939 Über eine experimentell beobachtete Erscheinung an Wirbelringen bei ihrer translatorischen Bewegung in wirklichen Flüssigkeiten. *Ann. Phys.* **5**, 497–523.

LANDMAN, M. J. & SAFFMAN, P. G. 1987 The three-dimensional instability of strained vortices in a viscous fluid. *Phys. Fluids* A **30**, 2339–2342.

MARSHALL, J. S. 1992 The effect of axial stretching on the three-dimensional stability of a vortex pair. *J. Fluid Mech.* **241**, 403–419.

MARSHALL, J. S. 1993 The effect of axial pressure gradient on axisymmetrical and helical vortex waves. *Phys. Fluids* A **5**, 588–599 (see also erratum, *Phys. Fluids* A **5**, 1857).

MAXWORTHY, T. 1972 The structure and stability of vortex rings. *J. Fluid Mech.* **51**, 15–36.

MAXWORTHY, T. 1974 Turbulent vortex rings. *J. Fluid Mech.* **64**, 227–239.

MAXWORTHY, T. 1977 Some experimental studies of vortex rings. *J. Fluid Mech.* **81**, 465–495.

SAFFMAN, P. G. 1992 *Vortex Dynamics.* Cambridge University Press.

SMITH, T. B. & BEESMER, K. M. 1959 Contrail studies of Jet Aircraft. *ASTIA AD* 217 188, April. Meteorology Research Inc. Pasadena, California, USA.

SPREITER, J. R. & SACKS, A. H. 1951 The rolling up of the trailing vortex sheet and its effect on downwash behind wings. *J. Aeronaut. Sci.* **18**, 21–32.

THOMAS, P. 1988 Experimentelle Untersuchung von Stabwirbeln in Wasser. *Rep.* 15/1988. Max-Planck-Institut für Strömungsforschung, Göttingen, Germany.

TSAI, C.-Y. & WIDNALL, S. E. 1976 The stability of short waves on a straight vortex filament in a weak externally imposed strain field. *J. Fluid Mech.* **73**, 721–733.

VAN DYKE, M. 1982 *An Album of Fluid Motion.* Stanford: Parabolic Press.

WIDNALL, S. E. 1975 The structure and dynamics of vortex filaments. *Ann. Rev. Fluid Mech.* **7**, 141–165.

WIDNALL, S. E., BLISS, D. B. & TSAI, C.-Y. 1974 The instability of short waves on a vortex ring. *J. Fluid Mech.* **66**, 35–47.

WIDNALL, S. E. & TSAI, C.-Y. 1977 The instability of the thin vortex ring of constant vorticity. *Phil. Trans. R. Soc. Lond.* A **287**, 273–305.